Resonance enhanced multiphoton ionisation spectroscopy of carbonyl sulphide

Morgan, R.A.; Baldwin, M.A.; Orr-Ewing, A.J.; Ascenzi, D.; Ashfold, M.N.R.; Buma, W.J.; Scheper, C.R.; de Lange, C.A.

DOI
10.1063/1.472088

Publication date
1996

Published in
Journal of Chemical Physics

Resonance enhanced multiphoton ionization spectroscopy of carbonyl sulphide

Ross A. Morgan, Andrew J. Orr-Ewing, Daniela Ascenzi,[a] and Michael N. R. Ashfold
School of Chemistry, University of Bristol, Bristol BS8 1TS, United Kingdom

Wybren Jan Buma, Connie R. Scheper, and Cornelis A. de Lange
Laboratory for Physical Chemistry, University of Amsterdam, Nieuwe Achtergracht 127, 1018 WS Amsterdam, The Netherlands

(Received 25 March 1996; accepted 30 April 1996)

Rydberg excited states of the OCS molecule in the energy range 70500–86000 cm^{-1} have been investigated via the two and three photon resonance enhancements they provide in the mass resolved multiphoton ionization (MPI) spectrum of a jet-cooled sample of the parent molecule. Spectral interpretation has been assisted by companion measurements of the kinetic energies of the photoelectrons that accompany the various MPI resonances. The present study supports the earlier conclusions of Weinkauf and Boesl [J. Chem. Phys. **98**, 4459 (1993)] regarding five Rydberg origins in the 70500–73000 cm^{-1} energy range, attributable to, respectively, states of $^3\Pi$, $^1\Pi$, $^3\Delta$, $^1\Delta$ and $^1\Sigma^+$ symmetry arising from the $4p\lambda \leftarrow 3\pi$ orbital promotion. We also identify a further 21 Rydberg origins at higher energies. These partition into clumps with quantum defects ca. 3.5 and 4.5, which we associate with the orbital promotions $np\lambda \leftarrow 3\pi$ ($n=5,6$), and others with near integer quantum defect which are interpretable in terms of excitation to s,d and (possibly) f Rydberg orbitals. We also identify MPI resonances attributable to $CO(X\ ^1\Sigma^+)$ fragments and to S atoms in both their ground (^3P) and excited (^1D) electronic states. Analysis of the former resonances confirms that the $CO(X)$ fragments resulting from one photon dissociation of OCS at excitation wavelengths ca. 230 nm are formed with a highly inverted, bimodal rotational state population distribution, whilst the latter are consistent with previous reports of the wavelength dependence for forming ground and excited state S atoms in the near uv photolysis of OCS. © *1996 American Institute of Physics.* [S0021-9606(96)01130-0]

INTRODUCTION

The spectroscopy[1–11] and photochemistry[7,12–20] of the excited electronic states of the 16 valence electron triatomic molecule carbonyl sulphide, OCS have both been the subject of much previous study. It has a linear ground state, with normal mode vibrational frequencies:[3] ν_1 (σ^+ symmetry, largely C–O stretch), 2062 cm^{-1}; ν_2 (π, bend), 520 cm^{-1} and ν_3 (σ^+, C–S stretch), 859 cm^{-1}, and an electronic configuration

$$\cdots(8\sigma)^2(2\pi)^4(9\sigma)^2(3\pi)^4;\tilde{X}\ ^1\Sigma^+. \tag{1}$$

The highest occupied 3π orbital is largely concentrated on the terminal sulphur atom, but the photoelectron spectrum[21–23] shows activity in ν_3 and, to a lesser extent, in ν_1, pointing to its having some antibonding character. Photoelectron spectroscopy (PES)[21–25] and photoionisation studies[26] give a value of 11.1736 ± 0.0015 eV (90121 ± 12 cm^{-1})[26] for the ionisation threshold for forming the lower ($^2\Pi_{3/2}$) spin–orbit state of the OCS^+ ion and a spin–orbit splitting (ca. 47 meV, 368 cm^{-1}) in good agreement with that deduced from analysis of the $OCS^+(\tilde{A}-\tilde{X})$ laser induced fluorescence (LIF)[27–29] and the laser induced fragmentation spectra of OCS^+.[30] Frequencies for the ground state ion stretching vibrations are well established: $\nu_1\sim2080$ cm^{-1} and $\nu_3\sim698$ cm^{-1}. The frequency of the bending mode, ν_2, has proven harder to define, with reported values ranging from 417 cm^{-1} [21] to 510 cm^{-1}.[24] The present work fully supports the lower value.

The lower lying valence excited states of OCS arising from the $4\pi\leftarrow3\pi$ and/or $10\sigma\leftarrow3\pi$ electron promotion have been studied by conventional absorption techniques[1–3,5,6,8] and the broad continua centred around 222, 167, and 152 nm assigned in terms of $^1\Delta\leftarrow\tilde{X}\ ^1\Sigma^+$, $^1\Pi\leftarrow\tilde{X}\ ^1\Sigma^+$ and $^1\Sigma^+\leftarrow\tilde{X}\ ^1\Sigma^+$ transitions, respectively. Studies of the temperature dependence of the longest wavelength absorption profile[31] led to the conclusion that the $^1\Delta$ excited state has a bent equilibrium geometry. Such a suggestion has been fully vindicated by more recent studies of the energy disposal and vector correlations amongst the primary photodissociation products—ground state CO molecules (carrying little vibrational excitation but with a highly inverted rotational state population distribution) together with excited $S(^1D)$ atoms.[16,17,19] The structured absorption centered around 152 nm shows a progression with a ca. 800 cm^{-1} interval.[6,9] This structure has been attributed to an unstable periodic orbit on the excited $^1\Sigma^+$ surface;[20] the anisotropy parameter ($\beta\sim1.8$) measured for the dominant primary products resulting from the 157 nm photolysis of $OCS-CO(X)$ molecules (in vibrational levels $v=0-3$, with comparatively modest levels of rotational excitation) and $S(^1S)$ atoms—serves to confirm

[a]Permanent address: Dipartimento di Chimica dell'Universita, Via Elce di Sotto, 8 1-06123 Perugia, Italy.

the parallel character of the photoexcitation process and the very short excited state lifetime.[18]

Absorption at shorter wavelengths is dominated by transitions to Rydberg states of OCS. The 70000–75000 cm^{-1} region has been studied extensively by one photon absorption spectroscopy,[1–6] electron energy loss spectroscopy[8] and, most recently, by resonance enhanced multiphoton ionisation (REMPI) spectroscopy.[10,11] Yang *et al.*[10] identified two-photon resonances associated with three Rydberg states in this region: the $\tilde{E}$ and $\tilde{F}$ states, both of which, following Kopp,[4] they labelled as having $^1\Pi$ symmetry, and the so-called $\tilde{P}$ state. This same region was investigated further by Weinkauf and Boesl,[11] who combined 2+1 and 3+1 MPI with careful measurements of the kinetic energies of the accompanying photoelectrons. Five Rydberg states were identified, all attributable to the electron promotion $4p\lambda \leftarrow 3\pi$, and a number of revisions of earlier analyses[4,10] were suggested. To date there do not appear to have been any reported multiphoton spectra involving the higher energy Rydberg states of OCS, but previous one photon absorption studies,[1–6] most notably that of Matsunaga and Watanabe,[5] have identified higher members of two Rydberg series converging to the two spin–orbit components of the ground state ion.

Here, we report the first comprehensive study of the entire two and three photon resonance enhanced MPI spectrum of a jet-cooled sample of OCS up to ca. 86000 cm^{-1}. Companion high resolution REMPI-PES measurements aid assignment of the numerous observed resonances, enabling confirmation of the conclusions reached by Weinkauf and Boesl[11] and the identification of a further 21 origins (and much attendant vibronic structure), all of which we associate with Rydberg states built on the ground state ion core. The present study of the OCS molecule complements our recent REMPI and REMPI-PES studies of the isoelectronic molecules CO_2[32] and CS_2[33] but, because of its lower symmetry and the absence of the u/g parity restrictions, assignment of the numerous OCS resonances in terms of excitations to specific Rydberg orbitals is necessarily less definitive.

EXPERIMENT

The results reported here were obtained using two complementary experimental systems: In Bristol, a home-built time-of-flight (TOF) mass spectrometer was used to record mass resolved REMPI spectra of jet-cooled OCS, and in Amsterdam REMPI-PES studies were performed using a ''magnetic bottle'' spectrometer. The latter experiment has been described in detail previously,[32–35] and only a cursory description is given here, but the Bristol TOF mass spectrometer is newly constructed and replaces our previous REMPI-TOF experiment, so is described in more detail.

The mass-resolved REMPI spectra [monitoring m/z 60 (OCS), 32 (S) and 28 (CO)] were recorded using a newly constructed (Wiley–McLaren configuration[36]) linear TOF mass spectrometer. The spectrometer consists of two acceleration stages and a field-free flight tube, and is housed within a high vacuum system consisting of two differentially pumped chambers connected by a small hole. The first chamber is pumped by a 150 mm diameter oil diffusion pump (Edwards Diffstak; chamber base pressure ca. 2×10^{-7} Torr) and contains a repeller and an extractor plate (diameters 100 and 125 mm, respectively), separated by a distance of 26 mm and, under typical working conditions, held at +400 and −400 V, respectively. A 25 mm diameter hole in the extractor plate, covered by 85% transmission nickel mesh (Buckbee–Mears) allows passage of any ions formed by REMPI between the extractor and repeller plates into the second acceleration region and the flight tube. The plate dividing the two vacuum chambers forms the front end of the field-free flight tube. It is 23 mm distant from the extractor plate, and has a 5 mm diameter hole covered with the 85% transmission mesh at its centre to pass the ions. This plate and the flight tube are normally held at −1400 V. The second vacuum chamber houses the 600 mm long flight tube, which is constructed of perforated stainless steel sheet. This chamber is pumped by a turbomolecular pump (Edwards EXT 501), and reaches a base pressure of ca. 7×10^{-8} Torr, which rises to 1×10^{-6} Torr when the experiment is operational. Ions exiting the flight tube through a 25 mm diameter hole covered with the same 85% transmission nickel mesh are detected by a pair of 25 mm diameter, chevron-configuration microchannel plates (Galileo).

A pulsed nozzle (General Valve Series 9) located between the repeller and extractor plates injects the gas of interest (here OCS, seeded 10% in Ar) into the first chamber. A series of suitably biased thin steel strips located close beneath the nozzle shield the electric field within the ionization region from the perturbing effects of the metal nozzle, but are small enough not to affect the gas expansion. The voltages on the steel strips are determined by a chain of matched resistors and maintain the linearity of the electric field lines in the extraction region. The gas pulse is intersected by a focused laser beam which drives the MPI process. A Nd:YAG pumped dye laser system (Spectra Physics GCR-230-10 and Lumonics HD-500, operating at 10 Hz repetition rate) is used to generate the laser pulses, with the dye laser output frequency-doubled in BBO or KDP crystals when necessary, and focused into the vacuum chamber by a 200 mm focal length quartz lens.

The output signal from the microchannel plates is accumulated by a digital oscilloscope (LeCroy 9361) and downloaded to a computer (486-PC, 50 MHz) via a GPIB interface for subsequent analysis. Mass resolved MPI spectra are obtained by scanning the dye laser wavelength continuously and monitoring just that fraction of the total ion signal with a TOF appropriate to the mass of interest, averaging typically 5–10 laser shots for each data point.

The REMPI-PES spectra were obtained in Amsterdam using an excimer pumped dye laser system with the laser output being frequency doubled when required, and focused (f.l. 25 mm) into the ionisation region of the magnetic bottle electron spectrometer. An effusive beam of pure OCS was used, and the resolution of the kinetic-energy resolved photoelectron spectra was typically 15 meV. Sulphur atoms were produced in the photolysis of OCS as a by product of the REMPI process. The measured electron kinetic energies

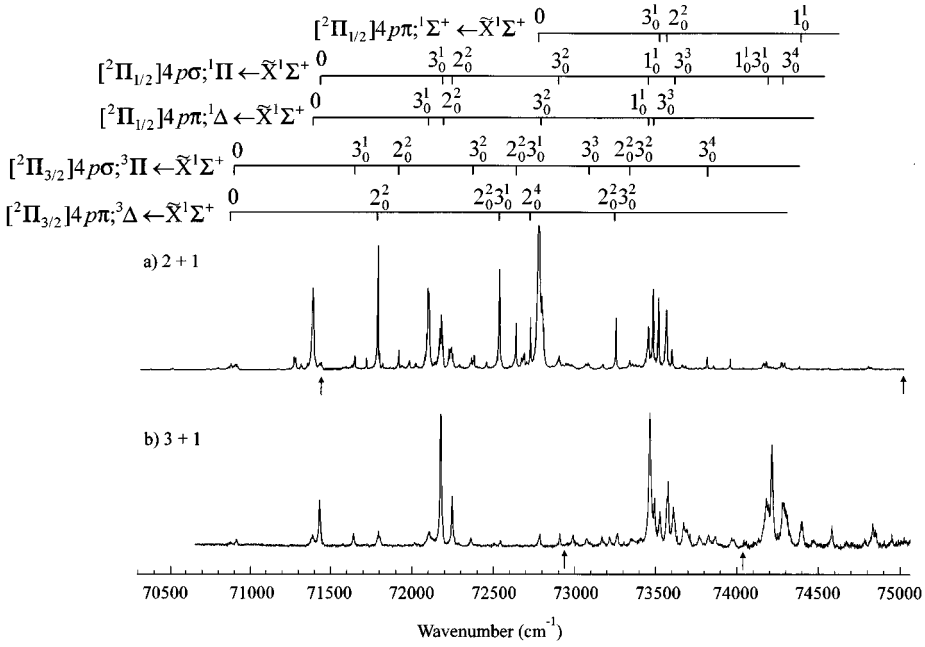

FIG. 1. (a) 2+1 and (b) 3+1 REMPI spectra of a jet-cooled sample of OCS over the energy range 70300–75000 cm^{-1} recorded using linearly polarized light and monitoring only those ions with TOFs appropriate to m/z 60. This spectrum is a composite, obtained by splicing together spectra recorded using more than one dye. The vertical arrows arranged below the respective spectra indicate where the various scans have been joined. No effort was made to ensure correct normalization of the relative intensities of features appearing within the tuning range of any one dye, or between one dye tuning curve and the next. Vibronic features associated with the various $[^2\Pi]4p\lambda \leftarrow \tilde{X}\ ^1\Sigma^+$ Rydberg states identified in Tables I and II are indicated via the combs superimposed above the spectrum.

from known S atom transitions provided a convenient calibration that enabled the OCS photoelectron kinetic energies to be placed on an absolute scale. In addition, xenon was used as a calibration gas. Certain wavelength-resolved REMPI spectra were also recorded in Amsterdam by mass-resolved ion detection or by measuring the total photoelectron yield as a function of excitation wavelength.

RESULTS AND DISCUSSION

REMPI spectra

Given a value of 90121 cm^{-1} for the first ionization limit of OCS[26] we can calculate that the long wavelength thresholds for four photon and three photon ionization of this molecule are, respectively, 444 and 333 nm. We have thus recorded REMPI spectra of OCS using linearly polarized laser radiation throughout the entire wavelength range 444−230 nm. These are shown in Figs. 1–3. As detailed in the figure captions, these spectra were recorded in one or other, or both, of two ways—either using a jet-cooled sample, with time-of-flight mass selection of the resulting ions (in Bristol), or using a thermal effusive source with mass selected ion, or kinetic energy selected photoelectron, detection (in Amsterdam). Inevitably, a number of different laser dyes were used in recording these spectra. The relative intensities of distant peaks should therefore be viewed with some caution since we have not taken any particular care to power normalize either between dyes or within the tuning range of any one dye. A few general points merit comment before embarking on any detailed discussion of these spectra. As Figs. 1–3 show, most of the excited state levels that show strongly in the 2+1 REMPI spectrum [panel (a) in Figs. 1–3] can be discerned via 3+1 REMPI spectroscopy [panel (b)] also, and vice versa, though on occasion their relative intensities show quite dramatic variations. Figure 4, which shows MPI spectra involving resonances in the 71000–72000 cm^{-1} region in much greater detail, provides one rather striking illustration of this point. The parallels between the 2+1 and 3+1 REMPI spectra of OCS reported here are in marked contrast to our recent REMPI investigation of the related molecule, CS_2.[33] This is simply a reflection of the fact that CS_2 is centrosymmetric, whilst OCS is not. As a result, symmetry imposes far fewer restrictions on the allowed electronic excitations in the latter molecule. Where comparisons are available, the wavenumbers of the resonances evident in Figs. 1–3 are in good agreement with those observed in previous one photon absorption,[1–6] electron energy loss[8] and/or multiphoton studies.[10,11] This is illustrated in Table I, which provides a complete listing of the wave numbers of all of the significant resonances we have identified in the 2+1 and 3+1 REMPI spectra of OCS.

The effects of OCS fragmentation manifest themselves in these spectra in several ways. Figure 3 highlights the paucity and weakness of features in the 2+1 REMPI spectrum for forming parent ions (m/z 60) at excitation wavelengths shorter than ca. 245 nm ($2\tilde{\nu} > 81500$ cm^{-1}). This approximates to the long wavelength end of the region of continuous uv absorption assigned in terms of excitation to the (bent) $^1A'$ and (linear) $^1A''$ Renner–Teller components of a disso-

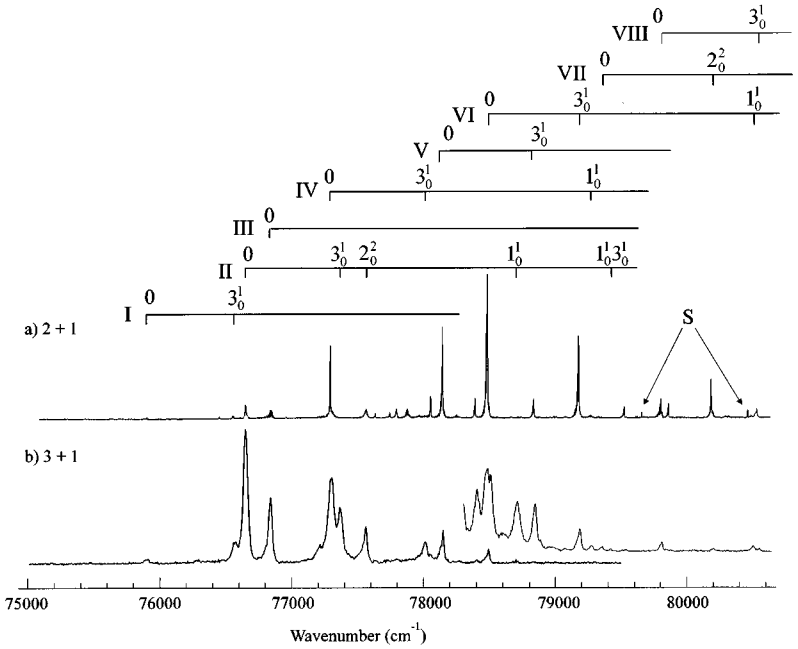

FIG. 2. Linearly polarized (a) 2+1 and (b) 3+1 REMPI spectra of OCS in the energy range 75000–80500 cm^{-1}. (a) was recorded using a jet-cooled sample, the entire tuning range of a single dye (coumarin 500) and monitoring the wavelength dependence of the m/z 60 signal. (b) was obtained using a thermal effusive source of OCS, again monitoring the parent ion yield save for the expanded view of the high frequency end of this spectrum which was obtained by monitoring the total photoelectron current. As with Fig. 1, the 3+1 REMPI spectrum is a composite obtained by splicing together spectra recorded using a number of different dyes, and the same comments apply. Vibronic features associated with the various Rydberg states identified in Tables I and II are indicated via the combs festooned above the spectra, whilst interfering resonances associated with neutral sulphur atoms in (a) are indicated by the symbol S.

ciative valence excited state which, in the linear limit, has $^1\Delta$ symmetry;[6,7,31] the weakness of the REMPI spectrum involving these shorter excitation wavelengths is attributable to this competing population loss channel at the energy of one absorbed photon. Several groups have studied the photochemistry of OCS following uv excitation in the wavelength range 220–250 nm and shown the primary products to be $S(^1D)$ atoms and $CO(X)$ fragments carrying substantial rotational excitation.[16,17,19] Consistent with this, our simultaneous investigation of the REMPI of S atoms suggests exclusive formation of $S(^1D)$ atoms in this range of excitation wavelengths. Figure 5 shows a part of the spectrum for forming ions with m/z 28 following one color excitation of OCS at wavelengths ca. 230 nm. This spectrum, which is readily assignable in terms of the well documented MPI spectrum of $CO(X)$, resonance enhanced at the two photon energy by the zero-point level of the $B\ ^1\Sigma^+$ state,[19] provides confirmation of the importance of this fragmentation channel under the present experimental conditions and of the highly excited, bimodal rotational state population distribution in the resulting $CO(X)$ photofragments. Note the appearance of the weak O and S branches in this spectrum, associated with the second rank $[T_0^2(\mathbf{A})]$ component of the two photon transition tensor. In the same vein, we suggest that the weakness of the m/z 60 signal in the 3+1 REMPI spectrum at excitation wavelengths less than ca. 352 nm ($3\tilde{\nu} > 85000\ cm^{-1}$) is likely due to competitive population loss via predissociation from the $^1\Pi$ excited state resonant at the two photon energy.[6,9,12,20]

REMPI-photoelectron spectra

The available experimental resolution (ca. 15 meV, 120 cm^{-1}) is sufficient to allow us to identify not just the vibrational, but also the spin–orbit, structure of the ions formed in the various REMPI processes. As has been demonstrated many times previously, the analysis of such spectra can provide considerable insight into the electronic and vibronic characteristics of the intermediate state providing the resonance enhancement. Figures 6–8 show a number of representative REMPI-PE spectra. All those selected for display arise as a result of three photon resonant, four photon ionisation processes. Consider first the spectrum shown in Fig. 6(a), recorded at a laser wavelength of 395.3 nm ($3\tilde{\nu} = 75897\ cm^{-1}$). The kinetic energy of the larger, faster peak is entirely consistent with ionisation to the $v^+ = 0$ level of the lower ($^2\Pi_{3/2}$) spin–orbit component of the ion, but the presence of a slower peak indicates that there is also some propensity for ionisation to the $v^+ = 0$ level of the higher ($^2\Pi_{1/2}$) state of the ion. Figures 6(b) and 6(c), obtained following excitation at wavelengths of 391.4 and 412.2 nm ($3\tilde{\nu} = 76650$ and $72777\ cm^{-1}$, respectively), show two further examples in which the final one photon ionization leads to formation of vibrationless ($v^+ = 0$) ions in both spin–orbit states. In both these cases, however, the higher ($^2\Pi_{1/2}$) component is observed to make the dominant contribution. Franck–Condon considerations, together with the apparent simplicity of all three of these spectra, lead us to conclude that, in each case, REMPI proceeds via an electronic (Ryd-

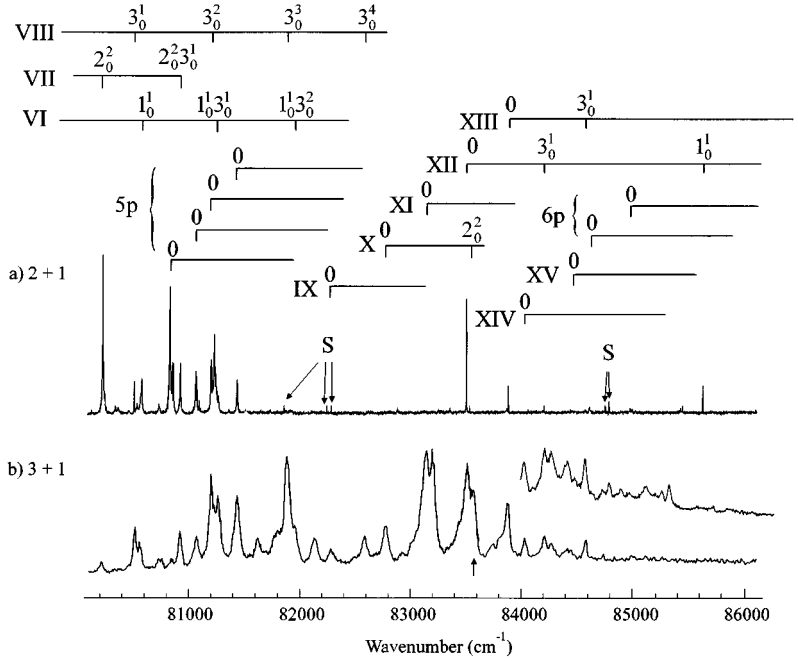

FIG. 3. Linearly polarized (a) 2+1 and (b) 3+1 REMPI spectra of OCS in the energy range 80200–86000 cm^{-1}, each recorded in the same manner as described in the caption to Fig. 2. Both displayed spectra are composites, obtained by splicing together spectra recorded using a number of different dyes, and the same reservations above relative peak intensities apply. The vertical arrows arranged below the respective spectra indicate where the various scans have been joined. Vibronic features associated with the various Rydberg states identified in Tables I and II are indicated via the combs arranged above the spectra, whilst interfering resonances associated with neutral sulphur atoms in (a) are indicated by the symbol S.

berg) origin level—albeit ones that, in every case, have a somewhat ''mixed'' spin–orbit core. These findings, and those derived from similar analyses of the REMPI-PE spectra accompanying virtually all other significant resonances in the 2+1 and 3+1 REMPI spectra of OCS [including those shown in Figs. 7 and 8 (see below)], are collected together in Table I.

Figures 7 and 8 provide further illustrations of the way in which REMPI-PES can be used to aid in the vibronic assignment of the resonance enhancing states. Figure 7(a), obtained monitoring photoelectrons at an excitation wavelength of 375.9 nm ($3\tilde{\nu}=79812\ cm^{-1}$), provides yet another example of ionisation occurring to the $v^+=0$ level of the ground state ion, predominantly the $^2\Pi_{1/2}$ spin–orbit component in this case. Figures 7(b) and 7(c), in contrast, show REMPI-PE spectra in which the peaks appear at kinetic energies lower than that predicted for formation of $v^+=0$ ions, indicating that the accompanying ions are formed with nonzero internal energy. The PE spectrum shown in Fig. 7(b), recorded at 372.6 nm ($3\tilde{\nu}=80508\ cm^{-1}$), exhibits two peaks with kinetic energies of 2.005 and 2.052 eV. These energies imply that the accompanying ions are formed in both the $^2\Pi_{3/2}$ and $^2\Pi_{1/2}$ spin–orbit states with, in each case, ca. 690 cm^{-1} of internal energy. This energy accords well with previous measurements of the ν_3 C–S stretching mode in the ion,[24,25] and we assign it as such. Franck–Condon considerations then suggest that the excited level of the neutral providing the resonance enhancement at 80508 cm^{-1} likely also carries one quantum of ν_3. Such is entirely consistent with experimental observation: A very similar energy interval (696 cm^{-1}) separates the 80508 cm^{-1} resonance from the 79812 cm^{-1} band which Fig. 7(a) showed unequivocally to be an electronic origin. Similar arguments operate in the case of the PE spectrum shown in Fig. 7(c), recorded at 366.4 nm ($3\tilde{\nu}=81882\ cm^{-1}$). The dominant feature here is consistent with the formation of ground state OCS^+ ions with a $^2\Pi_{1/2}$ core and ca. 2090 cm^{-1} of vibrational energy—an energy gap that accords well with the interval between the MPI resonance in question and the 79812 cm^{-1} origin. We can envisage two possible explanations for an energy separation of this size—either one quantum of the excited state ν_1 (C–O stretch) vibration or three quanta of ν_3. Both interpretations have some merit; it may well be that both contribute, and that their energy difference falls inside our available resolution.

Our final three examples (Fig. 8) involve the resonances observed at laser excitation wavelengths of 423.2, 417.9, and 412.5 nm ($3\tilde{\nu}=70881$, 71786, and 72726 cm^{-1}, respectively). The REMPI-PE spectrum associated with the first of these [Fig. 8(a)] is dominated by a peak whose kinetic energy (0.545 eV) is consistent with formation of ground state ions in the lower $^2\Pi_{3/2}$ spin–orbit state, suggesting that the 70881 cm^{-1} resonance involves another electronic origin. Such a result accords with the conclusions of most recent analyses.[4–7,10,11] Three other peaks are discernible. The next fastest is consistent with formation of $^2\Pi_{1/2}$, $v^+=0$ ions. More interestingly, the two slower peaks (which indicate formation of ions with ca. 810 and 1640 cm^{-1} of internal energy, respectively) are most readily assigned in terms of $^2\Pi_{3/2}$ ions carrying, respectively, two and four quanta of ν_2

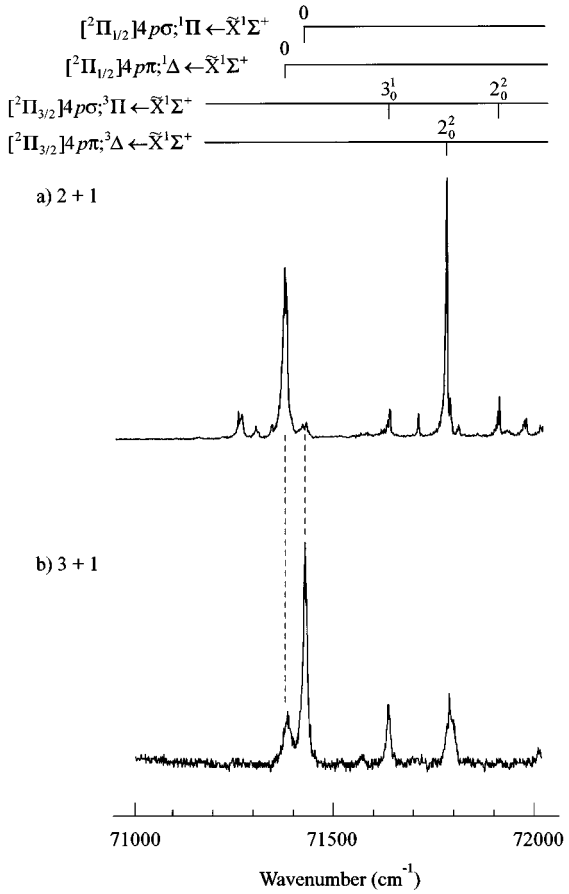

FIG. 4. Expanded view of (a) 2+1 and (b) 3+1 REMPI spectra of a jet-cooled sample of OCS in the energy range 71000–72000 cm^{-1} recorded using linearly polarized light and monitoring only those ions with TOFs appropriate to m/z 60. As the superimposed combs show, the former is dominated by vibronic features associated with the $[^2\Pi_{3/2}]4p\pi;^3\Delta \leftarrow \tilde{X}\ ^1\Sigma^+$ and $[^2\Pi_{1/2}]4p\pi;^1\Delta \leftarrow \tilde{X}\ ^1\Sigma^+$ transitions, whilst the $[^2\Pi_{1/2}]4p\sigma;^1\Pi \leftarrow \tilde{X}\ ^1\Sigma^+$ origin transition dominates the latter. See the text for some discussion of the strikingly different peak intensities in these two spectra.

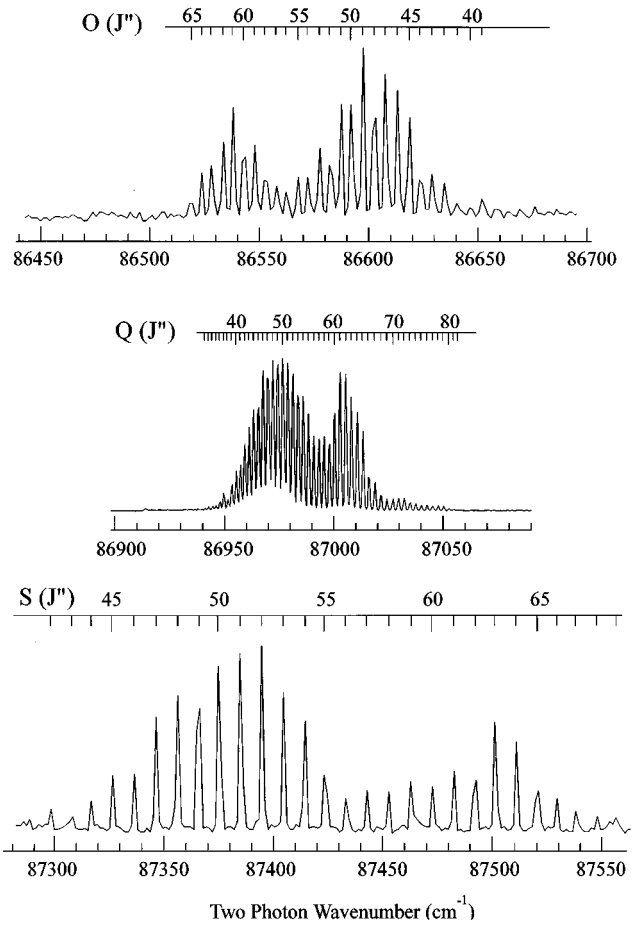

FIG. 5. 2+1 REMPI spectrum showing the origin band of the $B\ ^1\Sigma^+ \leftarrow X\ ^1\Sigma^+$ transition of the CO fragments formed by one photon dissociation of a jet-cooled sample of OCS at the same excitation wavelengths. Combs arranged above the spectrum indicate the dominant Q, and weak O and S, branches (the latter two plotted on a 30× expanded vertical scale) associated with the two photon transition and demonstrate the highly inverted, bimodal rotational state population distribution in the CO(X) photofragments.

bending excitation. Figures 8(b) and 8(c) serve to reinforce this conclusion. The former is dominated by a peak corresponding to formation of OCS^+ ions in their $^2\Pi_{3/2}$ spin–orbit state with ca. 810 cm^{-1} of internal energy. This internal energy, and the 905 cm^{-1} interval between the 70881 and 71786 cm^{-1} resonances, both encourage the interpretation that the resonance enhancement is provided by one (or more) of the Renner–Teller components associated with the 2^2 vibronic level of the state whose origin appears at 70881 cm^{-1}. The weaker features evident in Fig. 8(b) with kinetic energies of 0.695 and 0.54 eV are most sensibly assigned to ion formation in their $^2\Pi_{3/2}$, $v^+=0$ and $^2\Pi_{1/2}$, $v_2^+=2$ levels, respectively. In the same vein, the structure apparent in the REMPI-PE spectrum shown in Fig. 8(c) is most plausibly interpreted in terms of photoionisation to (in order of decreasing kinetic energy) the $^2\Pi_{3/2}$ and $^2\Pi_{1/2}$, $v_2^+=2$ levels and the $^2\Pi_{3/2}$ and $^2\Pi_{1/2}$, $v_2^+=4$ levels. Franck–Condon considerations suggest that the 72726 cm^{-1} resonance should be associated with one (or more) of the levels associated with the 2^4 vibronic level of the state originating at 70881 cm^{-1}. All of these assignments lend strong support to the lower ($\sim$417 cm^{-1}) of the values suggested for the ν_2 bending vibrational frequency in the ground state OCS^+ ion.[21]

Assigning the multiphoton resonances

Wave numbers ($\tilde{\nu}$) for the maxima of the various origin bands identified in this work are listed in Table II together with their effective quantum number [$(n^*=n-\delta)$, where n is the principal quantum number and δ the quantum defect] calculated using the relationship

$$\tilde{\nu} = E_i - R/(n^*)^2, \tag{2}$$

where R is the Rydberg constant (109737 cm^{-1}). The ionization limit, E_i, in this expression is taken as 90121 or 90500 cm^{-1}, according to whether the companion REMPI-PE spectrum identifies the Rydberg state as being associated with a series converging to the $^2\Pi_{3/2}$ or $^2\Pi_{1/2}$ spin–orbit component of the ion. For completeness, we also

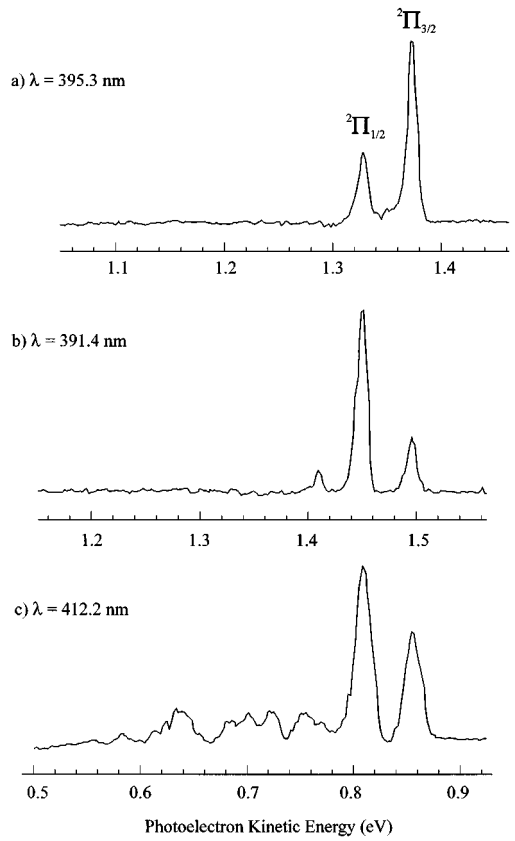

FIG. 6. Illustrative REMPI-PE spectra of OCS obtained following excitation at (a) 395.3 nm, where we excite a three photon resonance ($3\tilde{\nu}=75897$ cm^{-1}). The kinetic energy of the faster peak is consistent with ionization to the $v^+=0$ level of the lower spin–orbit component of the ion, whilst the slower peak indicates some propensity for ionisation to the $v^+=0$ level of the higher ($^2\Pi_{1/2}$) state also. (b) 391.4 nm ($3\tilde{\nu}=76650$ cm^{-1}); here the dominant peak indicates a propensity for forming ions in their ($^2\Pi_{1/2}$) $v^+=0$ level. (c) 412.2 nm ($3\tilde{\nu}=72777$ cm^{-1}). Our assignment of this three photon resonance in terms of the $[^2\Pi]4p\pi;{}^1\Sigma^+\leftarrow\tilde{X}\ {}^1\Sigma^+$ origin transition accords with the appearance of peaks indicating ionization to the $v^+=0$ level of both spin–orbit states of the ion. The kinetic energy scales have been offset so that the quantum states of the ion align vertically.

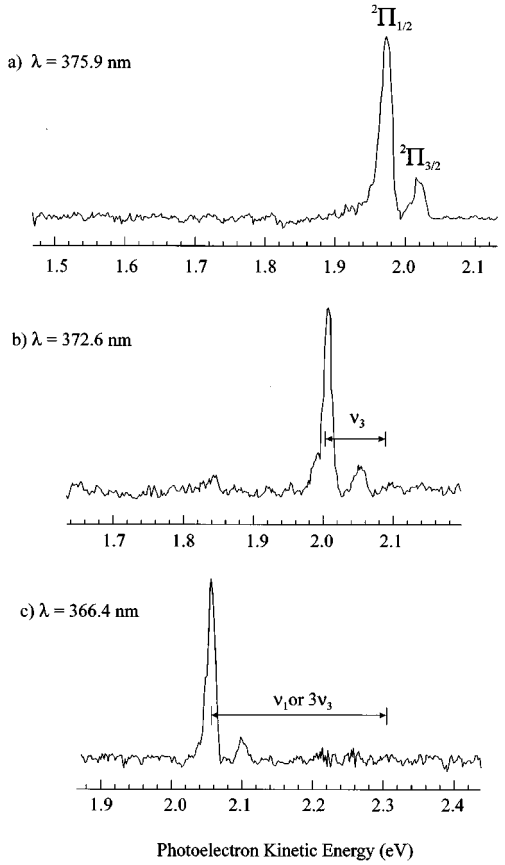

FIG. 7. REMPI-PE spectra of OCS obtained following excitation at (a) 375.9 nm ($3\tilde{\nu}=79812$ cm^{-1}), (b) 372.6 nm ($3\tilde{\nu}=80508$ cm^{-1}) and (c) 366.4 nm ($3\tilde{\nu}=81882$ cm^{-1}). On the basis of the measured photoelectron kinetic energies we deduce these three photon resonances involve, respectively, the origin, the 3_0^1 and the 3_0^3 and/or the 1_0^1 bands of a transition involving a Rydberg excited state built on a $[^2\Pi_{1/2}]$ ion core. As in Fig. 6, the kinetic energy scales have been offset so that the internal energy states of the ion align vertically.

indicate those resonances that have been identified in previous one photon absorption[1–6] and electron impact studies.[8]

The 70000–75000 cm^{-1} region shown in Fig. 1 has been the subject of many previous studies, including one high resolution absorption study[4] and two previous multiphoton investigations.[10,11] The five origins we identify in this region are consistent with the findings of Weinkauf and Boesl.[11] The companion REMPI-PE spectra allow us to deduce the dominant core configuration of each of these origins. The associated quantum defects ($\delta\sim1.5$–1.6, if we assume that $n=4$) suggest that all are first members of series arising from excitation to Rydberg orbitals with dominant p-character. The resonances at 70881 and 71385 cm^{-1}, evident in both 2+1 and 3+1 MPI spectroscopy and which the companion PE spectra show to involve, respectively, a $^2\Pi_{3/2}$ and a $^2\Pi_{1/2}$ ion core, have no obvious counterparts in the one photon absorption spectrum.[1–6] Following Weinkauf and Boesl,[11] it thus seems plausible to assign these two resonances in terms of the respective excitations $[^2\Pi_{3/2}]4p\pi;{}^3\Delta\leftarrow\tilde{X}\ {}^1\Sigma^+$ and $[^2\Pi_{1/2}]4p\pi;{}^1\Delta\leftarrow\tilde{X}\ {}^1\Sigma^+$. Here, as in our recent REMPI study of the Rydberg states of CS_2[33] we choose to indicate the upper state both in terms of a Hunds case (c) coupling scheme in which we specify the angular momentum of the ion core, Ω_c (3/2 or 1/2), along with the $nl\lambda$ character of the Rydberg electron, and in terms of the most appropriate Λ,S label, e.g., $^3\Delta$.

These two origins are in close coincidence with two other resonances, at 70911 and 71432 cm^{-1}. These latter resonances appear in both the 2+1 and 3+1 MPI spectra (Fig. 1) and in one photon absorption.[1–6] The associated REMPI-PE spectra indicate that these are origins, built on $^2\Pi_{3/2}$ and $^2\Pi_{1/2}$ ion cores, respectively. The quantum defects of these features suggest assignment in terms of a $4p\leftarrow\pi$ orbital excitation, whilst their one photon band contours[4] and their presence both in one photon absorption and in the multiphoton excitation spectra can be accommodated if we adopt the respective assignments $[^2\Pi_{3/2}]4p\sigma;{}^3\Pi\leftarrow\tilde{X}\ {}^1\Sigma^+$ and $[^2\Pi_{1/2}]4p\sigma;{}^1\Pi\leftarrow\tilde{X}\ {}^1\Sigma^+$. Such an assignment also accords with the conclusions of Weinkauf and Boesl,[11] is compatible with the earlier absorption work of Kopp[4] (who labelled

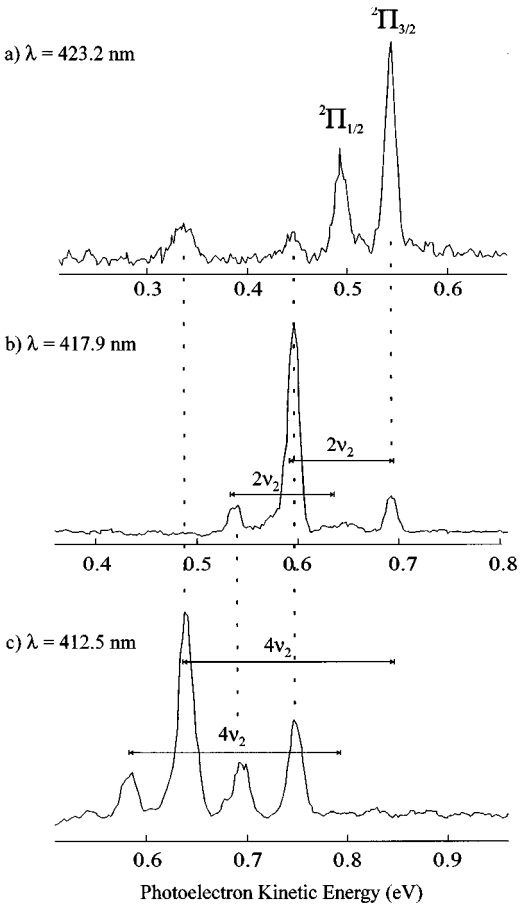

FIG. 8. REMPI-PE spectra of OCS obtained following excitation at (a) 423.2 nm ($3\tilde{\nu}=70881$ cm^{-1}), (b) 417.9 nm ($3\tilde{\nu}=71786$ cm^{-1}) and (c) 412.5 nm ($3\tilde{\nu}=72726$ cm^{-1}). The kinetic energy of the larger peak in (a) indicates the formation of $v^+=0$ ions in their lower spin–orbit state, consistent with assignment of this three photon resonance as the $[^2\Pi_{3/2}]4p\pi;^3\Delta\leftarrow\tilde{X}\ ^1\Sigma^+$ origin. The kinetic energies of the dominant peaks in (b) and (c) suggest that the 71786 and 72726 cm^{-1} resonances involve the 2_0^2 and 2_0^4 vibronic bands of this same Rydberg transition. As in Figs. 6 and 7, the kinetic energy scales in these PE spectra have been offset so that the internal energy states of the ion align vertically.

these respective origins in terms of excitations to the so-called $\tilde{E}$ and $\tilde{F}$ states), but contradicts the earlier multiphoton work of Yang *et al.*[10] Our final origin in this region, at 72777 cm^{-1}, appears in one photon absorption (but was not recognised as an origin in the only high resolution study of this feature[4]) and is assigned in terms of the only remaining dipole allowed transition associated with the orbital promotion $4p\pi\leftarrow\pi$, viz. the $^1\Sigma^+\leftarrow\tilde{X}\ ^1\Sigma^+$ transition involving an excited state traditionally labelled as the $\tilde{P}$ state.[10,11] The associated REMPI-PE spectrum [Fig. 6(c)] shows ''core mixing'' to be more developed in this particular excited state: it may be relevant to note that our recent REMPI-PES study of the Rydberg states of CS_2 revealed a similar high degree of core mixing in the Σ members of the $[^2\Pi]4p\pi$ Rydberg complex of this molecule also.[33] Again, as with CS_2, we are unable to identify any obvious candidate for the $[^2\Pi]4p\pi;^3\Sigma^-\leftarrow\tilde{X}\ ^1\Sigma^+$ counterpart of the 72777 cm^{-1} resonance. Weinkauf and Boesl[11] tentatively attributed a very weak feature at 70810 cm^{-1} in terms of this excitation but, unfortunately, its weakness precluded our being able to confirm or disprove such an origin assignment via REMPI-PES.

Several aspects of this spectral region merit further comment. The singlet–triplet splitting of both the Δ and Π Rydberg states we associate with the $4p\leftarrow\pi$ orbital promotion (504 and 521 cm^{-1}, respectively) are both substantially greater than the spin–orbit splitting of the ground state ion (ca. 368 cm^{-1}). This fact, and the observed core mixing revealed by the REMPI-PE spectra involving these states, can both be rationalized by appreciating that, as in the corresponding transitions of CS_2,[33] exchange interactions make a significant contribution to the observed splittings in these low n Rydberg states. For example, in the case of the two Π states, we can use the expression

$$K=\sqrt{\left(\frac{\Delta E}{2}\right)^2-A^2}, \tag{3}$$

where ΔE and A are, respectively, the observed singlet–triplet splitting (521 cm^{-1}) and the spin–orbit coupling constant appropriate to the ion core ($2A\sim368$ cm^{-1}), to estimate a value of 185 cm^{-1} for K, the exchange contribution to the observed splitting. As Table I showed, given the associated REMPI-PES data, it is possible to assign all remaining features in this region in terms of transitions involving excited vibronic levels built upon the various recognized origins. All three excited state vibrational modes are seen to be active in each of the more intense (singlet–singlet) transitions. The $^3\Delta\leftarrow\tilde{X}$ and, to a lesser extent, the $^1\Delta\leftarrow\tilde{X}$ transitions are noteworthy in as much that they exhibit more activity in the bending mode, and quite prominent resonances attributable in terms of various of the components of their respective 2_1^1 hot band transitions. This bending activity, and the change in bending frequency upon electronic excitation implied by the observed red shift of the 2_1^1 hot bands, suggests that the bending potentials for these excited states have a smaller curvature (around the linear equilibrium configuration) than that of the ground state neutral and the ion. Hopefully future *ab initio* calculations might be able to shed light on this observation, and also provide a rationale for the surprisingly low (cf. CS_2[33]) term values of these $^3\Delta$ and $^1\Delta$ Rydberg states *viz a viz* the Π states we attribute to the $4p\sigma\leftarrow\pi$ orbital promotion. We reserve discussion of the quite striking intensity variations shown by some of the resonances upon changing from 2+1 REMPI to 3+1 REMPI (as, for example, is illustrated in Fig. 4) until later.

Likely higher members of the various $np\leftarrow\pi$ Rydberg series are indicated in Figs. 2 and 3; the term values of the various origins and proposed assignments are listed in Table II. The companion REMPI-PE spectra show the 80850 and 81204 cm^{-1} features to involve Rydberg states with, respectively, $^2\Pi_{3/2}$ and $^2\Pi_{1/2}$ ion cores. Their quantum defects ($\delta\sim1.56$ assuming $n=5$) plus the fact that they are clearly apparent in the one photon absorption spectrum[5] encourages the respective assignments: $[^2\Pi_{3/2}]5p\sigma;^3\Pi\leftarrow\tilde{X}^1\Sigma^+$ and $[^2\Pi_{1/2}]5p\sigma;^1\Pi\leftarrow\tilde{X}\ ^1\Sigma^+$. The reduced ''singlet–triplet

TABLE I. Ion internal energies and vibronic assignments of multiphoton resonances observed in the two and three photon REMPI spectra (0=origin). Dominant photoelectron peaks are indicated in bold and the values in brackets represent the relative intensities of the peaks. Ion internal energies are deduced from the energy difference between the peak of interest in the REMPI-PE spectrum and that for formation of vibrationless $^2\Pi_{3/2}$ and $^2\Pi_{1/2}$ ions.

Wave number of resonance (cm^{-1})	Ion internal energy (in cm^{-1}) deduced from REMPI-PES		Proposed assignment of strongest vibronic feature
	$^2\Pi_{3/2}$ core	$^2\Pi_{1/2}$ core	
70741			2_2^2
70805			2_1^1
70881	**0** (10), 810 (1), 1650 (1)	0 (4)	0
71716			2_1^3
71786	0 (1), **810** (10)	840 (1)	2_0^2
72454			$2_1^3 3_0^1$
72534	850 (1), **1600** (10)	1620 (3)	$2_0^2 3_0^1$
72726	820 (4), **1630** (10)	810 (2), 1620 (2)	2_0^4
73175			$2_1^3 3_0^2$
73257			$2_0^2 3_0^2$
70911	**0** (10)	0 (2)	0
71645	**690** (10)	700 (2)	3_0^1
71915	0 (1), **850** (10)	820 (1)	2_0^2
72372	**1450** (10)	1420 (1)	3_0^2
72637			$2_0^2 3_0^1$
73071	**2060** (10), 1380 (1), 710 (1)	2060 (3)	3_0^3
73341			$2_0^2 3_0^2$
73757	**2770** (10)	2790 (2)	3_0^4
73809	2070 (5), **2900** (10)	2090 (2), 2930 (2)	$1_0^1 2_0^2$
71274			2_2^2
71312			2_1^1
71385	0 (2)	**0** (10)	0
72097	700 (1)	0 (1), **710** (10)	3_0^1
72171	700 (1), 800 (2)	0 (1), 710 (5), **810** (10), 1620 (1)	2_0^2
72796	0 (1), 1410 (2)	0 (2), 720 (1), **1400** (10)	3_0^2
73456	2050 (2)	**2050** (10)	1_0^1
73485	2120 (1)	**2120** (10)	3_0^3
71432	0 (3)	**0** (10)	0
72171	700 (1), 800 (2)	0 (1), **710** (5), 810 (10), 1620 (1)	3_0^1
72233	830 (2)	0 (1), **840** (10)	2_0^2
72902	1420 (3)	**1450** (10)	3_0^2
73456	2020 (4)	**2050** (10)	1_0^1
73594	2080 (4)	720 (1), 1420 (2), **2100** (10)	3_0^3
74177			$1_0^1 3_0^1$
74277	2770 (2)	**2800** (10), 2070 (1)	3_0^4
72777	0 (7)	**0** (10)	0
73519	710 (6)	**700** (10)	3_0^1
73566	840 (6), 2150 (2)	**870** (10), 2200 (6)	2_0^2
74814	2080 (7)	**2040** (10)	1_0^1
75897	**0** (10)	0 (3)	0
76578	0 (1), **690** (10)	680 (1)	3_0^1
76650	0 (3), 700 (1)	**0** (10)	0
77361	690 (2)	**710** (10)	3_0^1
77520	840 (3)	**860** (10)	2_0^2
78708	2020 (2)	**2020** (10)	1_0^1
79422	2760 (2)	2060 (1), **2740** (10)	$1_0^1 3_0^1$
76833	0 (4)	**0** (10), 830 (1)	0
77292	0 (4)	**0** (10)	0
78012	710 (4)	**710** (10)	3_0^1
79272	2040 (3)	**2040** (10)	1_0^1
78058			2_1^1
78144	**0** (10)	0 (1)	0
78852	**710** (10)	730 (1)	3_0^1
78395			2_1^1
78486	0 (1)	**0** (10)	0
79182	690 (1)	**690** (10)	3_0^1

TABLE I. (*Continued*).

Wave number of resonance (cm^{-1})	Ion internal energy (in cm^{-1}) deduced from REMPI-PES		Proposed assignment of strongest vibronic feature
	$^2\Pi_{3/2}$ core	$^2\Pi_{1/2}$ core	
80556	2030 (1)	**2040** (10)	1_0^1
79356	**0** (10)	0 (1)	0
80204	810 (4)	**1650** (10)	$2_0^2/2_0^4$
81900			$2_0^2 3_0^1$
79812	0 (2)	**0** (10)	0
80508	690 (1)	**690** (10)	3_0^1
81204	1370 (1)	0 (10), **1380** (10)	$0/3_0^2$
81882	2120 (1)	**2100** (10)	$1_0^1/3_0^3$
82584	2190 (1)	1460 (1), **2880** (10)	3_0^4
80850	**0** (10), 1530 (1)		0
81072	**0** (10), 1680 (1), 2900 (1)	0 (5)	0
81204	1370 (1)	**0** (10), 1380 (10)	$0/3_0^2$
81438	0 (2), 2080 (4)	**0** (10), 2080 (1)	0
82278	**0** (10)	0 (1)	0
82776	0 (1)	**0** (10)	0
83568	0 (1), 810 (4), 2460 (4)	0 (1), 850 (10), 2480 (10)	$2_0^2/2_0^6$
83148	0 (7), 810 (7), 2070 (7)	**0** (10), 2030 (7)	0
83514	**0** (10)	0 (1)	0
84207	**710** (10)	710 (1)	3_0^1
85634	**2080** (10)	2050 (2)	1_0^1
83874	0 (1), 1660 (1)	**0** (10)	0
84573	700 (1)	0 (1), **710** (10)	3_0^1
84030	**0** (10)		0
84411		**0** (10)	0
84627	**0** (10)		0
84996		**0** (10)	0

splitting'' (ca. 354 cm^{-1}, comparable with the spin–orbit splitting of the ion) and the much ''cleaner'' REMPI-PE spectrum (see Table I) both serve to illustrate the rapid evolution towards the expected Hund's case (c) limit with increasing n. The two other origins identified in this region, at 81072 and 81438 cm^{-1}, show a very similar splitting. Analogy with the $4p\leftarrow\pi$ Rydberg complex and the fact that these resonances have not been identified in one photon absorption leads us to propose the respective assignments $[^2\Pi_{3/2}]5p\pi;^3\Delta\leftarrow\tilde{X}\ ^1\Sigma^+$ and $[^2\Pi_{1/2}]5p\pi;^1\Delta\leftarrow\tilde{X}\ ^1\Sigma^+$. We note that such an assignment implies a reversal of the energetic ordering of the $\Pi(np\sigma\leftarrow\pi)$ and $\Delta(np\pi\leftarrow\pi)$ states on going from $n=4$ to $n=5$. Two resonances attributable to members of the $6p\leftarrow\pi$ complex are discernible, most notably in the 3+1 REMPI spectrum, with respective wave numbers 84627 and 84996 cm^{-1}. Given that these appear in one photon absorption also, it seems reasonable to suggest the respective assignments $[^2\Pi_{3/2}]6p\sigma;^3\Pi\leftarrow\tilde{X}\ ^1\Sigma^+$ and $[^2\Pi_{1/2}]6p\sigma;^1\Pi\leftarrow\tilde{X}\ ^1\Sigma^+$.

We identify a further fifteen electronic origins in the 75000–85000 cm^{-1} region (Figs. 2 and 3), most of which have no clear counterparts in the one photon absorption spectrum of OCS. We start by considering the pair of features at 78144 and 78486 cm^{-1} and their attendant vibronic structure (Table I), which dominate the 2+1 REMPI spectrum in this region and have been identified in one photon absorption also.[5] The companion REMPI-PE spectra prove that these are origins involving excited states with, respectively, a $^2\Pi_{3/2}$ and a $^2\Pi_{1/2}$ ion core; the peak separation (342 cm^{-1}) is actually slightly smaller than the spin–orbit splitting of the ground state ion. Their effective principal quantum numbers (both $n^*=3.02$, calculated relative to the appropriate ionisation limits) are compatible with assignment in terms of excitation to either a $3d$ or the $5s\sigma$ Rydberg orbital. It is likely that the pair of features at 83514 and 83874 cm^{-1} (which the REMPI-PE spectra confirm to be built on $^2\Pi_{3/2}$ and $^2\Pi_{1/2}$ ion cores, respectively) are the next spin–orbit split member of this Rydberg series, though we recognize that their quantum defect would also be compatible with a $4f\leftarrow\pi$ Rydberg assignment.

We identify a further six origins in the vicinity of the 78144 cm^{-1} feature, only one of which appears to have been identified in one photon absorption.[5] REMPI-PES shows the lowest energy resonance (at 75897 cm^{-1}) to involve a $^2\Pi_{3/2}$ core, whereas the next three (at 76650, 76833, and 77292 cm^{-1}) all involve the excited spin–orbit core. Assignment of any one of these three as the ''singlet'' partner of the 75897 cm^{-1} feature would imply an abnormally large exchange interaction. The 76650 cm^{-1} transition, and its associated vibronic features (Table I), shows particularly strongly in the 3+1 REMPI spectrum—behavior very reminiscent of that exhibited by the previously discussed $[^2\Pi_{1/2}]4p\sigma;^1\Pi\leftarrow\tilde{X}\ ^1\Sigma^+$ resonance at longer wavelength. REMPI-PE spectroscopy shows the two origins to higher energy (at 79356 and 79812 cm^{-1}) to involve $^2\Pi_{3/2}$ and $^2\Pi_{1/2}$ ion cores, respectively; both show n^* values ca. 3.2,

TABLE II. Wave numbers ($\tilde{\nu}$), effective quantum defects (n^*) and proposed assignments for the various origin bands assigned in the 2+1 and 3+1 REMPI spectra. Where no definite assignments are possible we list the spin–orbit component of the ion core and state number so as to allow identification in Figs. 1–3. Bands identified in previous one photon absorption (Refs. 2–5) and electron impact studies (in brackets) (Ref. 8) are also indicated.

$\tilde{\nu}$ (cm^{-1})	n^*	One photon	Assignment
70881	2.39		$[^2\Pi_{3/2}]4p\pi;^3\Delta\leftarrow\tilde{X}\ ^1\Sigma^+$
70911	2.39	70913[a]	$[^2\Pi_{3/2}]4p\sigma;^3\Pi\leftarrow\tilde{X}\ ^1\Sigma^+$
71385	2.40	(71395)	$[^2\Pi_{1/2}]4p\pi;^1\Delta\leftarrow\tilde{X}\ ^1\Sigma^+$
71432	2.40	71430[a,b]	$[^2\Pi_{1/2}]4p\sigma;^1\Pi\leftarrow\tilde{X}\ ^1\Sigma^+$
72777	2.49	72776[a] (72775)	$[^2\Pi_{1/2}]4p\pi;^1\Sigma^+\leftarrow\tilde{X}\ ^1\Sigma^+$
75897	2.78	75899[c]	$[^2\Pi_{3/2}]$; State I
76650	2.81		$[^2\Pi_{1/2}]$; State II
76833	2.83		$[^2\Pi_{1/2}]$; State III
77292	2.88	(77299)	$[^2\Pi_{1/2}]$; State IV
78144	3.02	78156[c]	$[^2\Pi_{3/2}]$; State V
78486	3.02	78497[c]	$[^2\Pi_{1/2}]$; State VI
79356	3.19		$[^2\Pi_{3/2}]$; State VII
79812	3.20		$[^2\Pi_{1/2}]$; State VII
80850	3.44	80840[b] (80849)	$[^2\Pi_{3/2}]5p\sigma;^3\Pi\leftarrow\tilde{X}\ ^1\Sigma^+$
81072	3.48		$[^2\Pi_{3/2}]5p\pi;^3\Delta\leftarrow\tilde{X}\ ^1\Sigma^+$
81204	3.44	81210[b] (81203)	$[^2\Pi_{1/2}]5p\sigma;^1\Pi\leftarrow\tilde{X}\ ^1\Sigma^+$
81438	3.48		$[^2\Pi_{1/2}]5p\pi;^1\Delta\leftarrow\tilde{X}\ ^1\Sigma^+$
82278	3.74		$[^2\Pi_{3/2}]$; State IX
82776	3.77		$[^2\Pi_{1/2}]$; State X
83148	3.86		$[^2\Pi_{1/2}]$; State XI
83514	4.07		$[^2\Pi_{3/2}]$; State XII
83874	4.07		$[^2\Pi_{1/2}]$; State XIII
84030	4.25		$[^2\Pi_{3/2}]$; State XIV
84411	4.25		$[^2\Pi_{1/2}]$; State XV
84627	4.47	84620[b] (84607)	$[^2\Pi_{3/2}]6p\sigma;^3\Pi\leftarrow\tilde{X}\ ^1\Sigma^+$
84996	4.47	84990[b]	$[^2\Pi_{1/2}]6p\sigma;^1\Pi\leftarrow\tilde{X}\ ^1\Sigma^+$

[a]Reference 4.
[b]Reference 5.
[c]Reference 2.

again hinting at an assignment in terms of excitation to a member of the $5s/3d$ Rydberg ''supercomplex.'' However, further speculation as to the symmetries of the excited states responsible for these various resonances, and what we presume to be the analogous set of origins in the energy region 82250–84500 cm^{-1}, is probably unwarranted given the large number of possible excited states in each region: i.e., $^3\Pi$ and $^1\Pi$ states from the excitation $ns\leftarrow\pi$ and from $nd\sigma\leftarrow\pi$, $^{3,1}\Sigma^+$, $^{3,1}\Sigma^-$ and $^{3,1}\Delta$ states from the promotion $nd\pi\leftarrow\pi$, and $^{3,1}\Pi$ and $^{3,1}\Phi$ states as a result of the excitation $nd\delta\leftarrow\pi$.

Finally we consider what can be gleaned from the relative intensities of the various REMPI features, and the way these vary depending upon whether a given state is viewed as a two or three photon resonance enhancement. The examples highlighted in Fig. 4 represents something of an extreme case. Obviously it is first necessary to establish that the observed differences are not in some sense an artefact, e.g., reflecting the presence of some hitherto unrecognised, accidentally resonant state at the one (or two) photon energy, or a consequence of different excited state lifetimes and the very different intensities used in exciting 2+1 and 3+1 REMPI spectra, or due to the fact that the spectra displayed in Fig. 4 were obtained by monitoring just the parent ion yield. We concur with previous workers[11] that none of these factors can explain the very different relative strengths observed for the $[^2\Pi_{1/2}]4p\sigma;^1\Pi\leftarrow\tilde{X}\ ^1\Sigma^+$ and $[^2\Pi_{1/2}]4p\pi;^1\Delta\leftarrow\tilde{X}\ ^1\Sigma^+$ resonances (Fig. 4). Weinkauf and Boesl[11] suggested an extension of the parity selection rule to argue that the $^1\Delta\leftarrow\tilde{X}\ ^1\Sigma^+$ transition should show strongly in two photon excitation, whilst $^1\Pi\leftarrow\tilde{X}\ ^1\Sigma^+$ transitions should be favored by one and three photon excitations (consistent with the observations in Fig. 4). Whilst such a propensity is frequently observed to hold for changes in the l quantum number in atoms and hydride molecules in which the HOMO is well approximated as an atomic orbital,[37] it is far from clear why it should apply to changes in the Λ quantum number in a molecule like OCS. Clearly angular momentum constraints exclude one photon $^1\Delta\leftarrow\tilde{X}\ ^1\Sigma^+$ transitions in a linear molecule, but we suspect that additional information (e.g., some knowledge of the composition of the various l functions contributing to the various low lying Rydberg orbitals) will be needed before one can offer a wholly convincing explanation as to why this particular $^1\Delta\leftarrow\tilde{X}\ ^1\Sigma^+$ resonance is favored by two photon excitation whilst the neighboring $^1\Pi\leftarrow\tilde{X}\ ^1\Sigma^+$ transition appears more strongly in 3+1 REMPI.

Fragmentation

The mass resolved REMPI spectra showed numerous resonances in the m/z 32 (S) mass channel and, as Fig. 5 showed, a few notable features in the m/z 28 (CO) mass channel also. The structured m/z 28 resonance observed at excitation wavelengths ca. 230 nm is readily attributable to MPI of ground state CO molecules, resonance enhanced at the two photon energy by the zero-point level of the $B\ ^1\Sigma^+$ state.[19] The highly excited, bimodal rotational state population distribution is consistent with previous measurements of the energy disposal in the $CO(X)$ fragments resulting from one uv photon dissociation of OCS at 230 nm[19] and 222 nm,[16,17] i.e., following excitation within its $^1\Delta\leftarrow\tilde{X}\ ^1\Sigma^+$ absorption system. Some signal attributable to S^+ ions was observed at all wavelengths where OCS undergoes 2+1 REMPI; this has been commented on previously,[11] and is attributable to one photon excitation and subsequent fragmentation of the ground state OCS^+ ions formed in the initial REMPI process. Of greater interest are the strong resonances appearing at excitation wavelengths less than ca. 260 nm, attributable to REMPI of neutral S atom fragments. We have been able to assign many, though by no means all, of these lines by referring to previous listings of S atom excited state term values.[38–40] (It is inappropriate to list the wave numbers of all of the observed resonances here, but a complete listing is available from the authors upon request). We see a clear dividing line at 251.5 nm. All assigned resonances at longer wavelength are attributable to two photon transitions originating from the ground (^3P) state, whilst at all shorter wavelengths we only identify two photon resonances associated with the excited (^1D) state. The latter observation is particularly significant, since the region down to

ca. 241 nm should be rich with two photon resonances originating from the ground state and involving triplet members of Rydberg series converging to the ground ($^4S^0$) state of the ion.[40] All of these observations are explicable in terms of known near uv photochemistry of OCS. The ground state atoms observed at the longest wavelengths (>251.5 nm) probably arise as a result of one photon absorption to (and dissociation from) triplet valence states which must contribute in this region of the near uv absorption spectrum of the parent, whilst the observed onset of the S(^1D) resonances marks the long wavelength limit of the much stronger parent $^1\Delta \leftarrow \tilde{X}\ ^1\Sigma^+$ absorption. The lack of (^3P) resonances at these shorter excitation wavelengths is consistent with previous reports[17,19] that the $^1\Delta$ state of the parent fragments to singlet products [CO(X)+S(^1D)] with a (near) unit quantum yield.

CONCLUSION

The present work reports the use of two and three photon resonant MPI spectroscopy to investigate Rydberg excited states of the OCS molecule in the energy range 70500–86000 cm^{-1}. Our interpretation of the various observed resonances has been greatly assisted by companion measurements of the kinetic energies of the accompanying photoelectrons. The present study serves to reinforce earlier conclusions[11] regarding five Rydberg origins in the 70500–73000 cm^{-1} energy range, which have been attributed to, respectively, states of $^3\Pi$, $^1\Pi$, $^3\Delta$, $^1\Delta$ and $^1\Sigma^+$ symmetry arising from the $4p\lambda \leftarrow 3\pi$ orbital promotion. At higher energies we identify no fewer than 21 more Rydberg origins. These appear in a number of clumps. Those with quantum defects ca. 3.5 and 4.5 we associate with the orbital promotions $np\lambda \leftarrow 3\pi$ ($n=5,6$), whilst the others with near integer quantum defect we suggest must be associated with excitation to s,d and (possibly) f Rydberg orbitals. We also identify a number of MPI resonances with m/z 28 and 32 which we attribute to, respectively, CO($X\ ^1\Sigma^+$) fragments and S atoms [in both their ground (^3P) and excited (^1D) electronic states]. Analysis of the former feature confirms that the CO(X) fragments resulting from one photon dissociation of OCS at excitation wavelengths ca. 230 nm are formed with a highly inverted, bimodal rotational state population distribution, whilst the latter are consistent with previous reports of the wavelength dependence for forming ground and excited state S atoms in the near uv photolysis of OCS.

ACKNOWLEDGMENTS

Once again the Bristol group is happy to acknowledge financial support from the EPSRC (previously SERC) in the form of equipment grants and a studentship (to R.A.M.), and the unstinting practical help and encouragement of Mr K. N. Rosser. A.J.O.-E. is grateful to the Royal Society for the award of the Eliz. Challenor Research Fellowship, whilst M.N.R.A. is grateful to the Ciba Fellowship Trust for their support of the Bristol-Amsterdam collaboration. D.A. acknowledges the financial support of the European Union Erasmus sheme. The Amsterdam group gratefully acknowledges the Netherlands Organization for Scientific Research (N.W.O.) for equipment grants and financial support.

[1] W. C. Price and D. M. Simpson, Proc. R. Soc., London Ser. A **169**, 50 (1939).
[2] Y. Tanaka, A. S. Jursa, and F. J. LeBlanc, J. Chem. Phys. **32**, 1205 (1960).
[3] G. Herzberg, *Molecular Spectra and Molecular Structure, Vol III. Electronic Spectra and Electronic Structure of Polyatomic Molecules* (Van Nostrand Reinhold, Princeton, 1966).
[4] I. Kopp, Can. J. Phys. **45**, 4011 (1967).
[5] F. M. Matsunaga and K. Watanabe, J. Chem. Phys. **46**, 4457 (1967).
[6] J. W. Rabalais, J. M. McDonald, V. Scherr, and S. P. McGlynn, Chem. Rev. **71**, 73 (1971).
[7] M. N. R. Ashfold, M. T. Macpherson, and J. P. Simons, Topics Curr. Chem. **86**, 1 (1979), and references therein.
[8] B. Leclerc, A. Poulin, D. Roy, M. J. Hubin-Franskin, and J. Delwiche, J. Chem. Phys. **75**, 5329 (1981).
[9] M. I. McCarthy and V. Vaida, J. Phys. Chem. **92**, 5874 (1988).
[10] B. Yang, M. H. Eslami, and S. L. Anderson, J. Chem. Phys. **89**, 5527 (1988).
[11] R. Weinkauf and U. Boesl, J. Chem. Phys. **98**, 4459 (1993).
[12] G. Black, R. L. Sharpless, T. G. Slanger, and D. C. Lorents, J. Chem. Phys. **62**, 4274 (1975).
[13] S. V. Filseth, Adv. Photochem. **10**, 1 (1977), and references therein.
[14] G. S. Ondrey, S. Kanfer, and R. Bersohn, J. Chem. Phys. **79**, 179 (1983).
[15] N. van Veen, P. Brewer, P. Das, and R. Bersohn, J. Chem. Phys. **79**, 4925 (1983).
[16] N. Sivakumar, I. Burak, W.-Y. Cheung, P. L. Houston, and J. W. Hepburn, J. Phys. Chem. **89**, 3609 (1985).
[17] N. Sivakumar, G. E. Hall, P. L. Houston, J. W. Hepburn, and I. Burak, J. Chem. Phys. **88**, 3692 (1988), and references therein.
[18] C. E. Strauss, G. C. McBane, P. L. Houston, I. Burak, and J. W. Hepburn, J. Chem. Phys. **90**, 5364 (1989).
[19] Y. Sato, Y. Matsumi, M. Kawasaki, K. Tsukiyama, and R. Bersohn, J. Phys. Chem. **99**, 16307 (1995).
[20] C. D. Pibel, K. Ohde, and K. Yamanouchi, J. Chem. Phys. **101**, 836 (1994).
[21] R. Frey, B. Gotchev, W. B. Peatman, H. Pollak, and E. W. Schlag, Int. J. Mass Spectrom. Ion Phys. **26**, 137 (1978).
[22] J. Delwiche, M. J. Hubin-Franskin, G. Caprace, P. Natalis, and D. Roy, J. Electron Spectrosc. Relat. Phenom. **21**, 205 (1980).
[23] J. Delwiche, M. J. Hubin-Franskin, P. M. Guyon, and I. Nenner, J. Chem. Phys. **74**, 4219 (1981).
[24] B. Kovac, J. Chem. Phys. **78**, 1684 (1983).
[25] L.-S. Wang, J. E. Reutt, Y. T. Lee and D. A. Shirley, J. Electron Spectrosc. Relat. Phenom. **46**, 167 (1988).
[26] Y. Ono, E. A. Osuch and C. Y. Ng, J. Chem. Phys. **74**, 1645 (1981).
[27] J. P. Maier and F. Thommen, Chem. Phys. **51**, 319 (1980).
[28] C. Y. R. Wu, T. S. Yih, and D. L. Judge, Int. J. Mass Spectrom. Ion Phys. **68**, 303 (1986).
[29] M. Tsuji and J. P. Maier, Chem. Phys. Lett. **137**, 421 (1987).
[30] R. Kakoschke, U. Boesl, J. Hermann, and E. W. Schlag, Chem. Phys. Lett. **119**, 467 (1985).
[31] J. A. Joens, J. Chem. Phys. **89**, 5366 (1985), and references therein.
[32] M. R. Dobber, W. J. Buma, and C. A. de Lange, J. Chem. Phys. **101**, 9303 (1994), and references therein.
[33] R. A. Morgan, M. A. Baldwin, A. J. Orr-Ewing, M. N. R. Ashfold, W. J. Buma, J. B. Milan, and C. A. de Lange, J. Chem. Phys. **104**, 6117 (1995), and references therein.
[34] B. G. Koenders, D. M. Wieringa, K. E. Drabe, and C. A. de Lange, Chem. Phys. **118**, 13 (1987).
[35] N. P. L. Wales, E. de Beer, N. P. C. Westwood, W. J. Buma, and C. A. de Lange, J. Chem. Phys. **100**, 7984 (1994).
[36] M. C. Wiley and I. H. McLaren, Rev. Sci. Instrum. **26**, 1150 (1955).
[37] M. N. R. Ashfold and J. D. Howe, Annu. Rev. Phys. Chem. **45**, 57 (1994), and references therein.
[38] W. C. Martin, R. Zalubas, and A. Musgrove, J. Phys. Chem. Ref. Data **19**, 821 (1990), and references therein.
[39] S. T. Pratt, Phys. Rev. A **38**, 1270 (1988).
[40] S. Woutersen, J. B. Milan, W. J. Buma, and C. A. de Lange (unpublished).